

In situ identification and quantification in a flow cell with AAS downstream analytics

Michael Voith · Gerald Luckeneder · Achim Walter Hassel

Received: 15 June 2012 / Revised: 14 September 2012 / Accepted: 16 September 2012 / Published online: 14 October 2012
© Springer-Verlag Berlin Heidelberg 2012

Abstract To broaden the application range of materials and the challenge of corrosion protection leads to the development of novel metal coatings. Therefore, an investigation of the reactions between the coating and different process media under laboratory conditions is necessary. In the current work, a system is established which allows a continuous in situ identification and quantification of the soluble species by coupling a flow-through cell with an atomic absorption spectrometer. Because of the cell design, it is also possible to observe surface changes and gas formation. To improve the process media flow through the cell and to reduce peak broadening of the analyte signal in the atomic absorption spectroscopy due to enlarged retention time of soluble species from interest, the cell geometry was adapted and the flow was simulated with a computational fluid dynamics software.

Keywords In situ determination · Flow cell · Flowing process media · Atomic absorption spectroscopy

Introduction

A detailed understanding of dissolution and corrosion processes can rely on the use of a single method only in very

simple cases. As soon as concurrent reactions take place or more complex materials such as alloys or coated materials are used a method combination may provide the required data to understand the underlying mechanism. As an example for the study of the dissolution or corrosion mechanism of an alloy in contact with changing process media, it is necessary to couple electrochemistry with multiple downstream analytical techniques. To obtain information about time dependencies of chemical reactions occurring during the contact of a sample surface with the flowing electrolyte, a flow cell connected with downstream analytics should be used. Ogle and Weber developed a flow cell to measure dissolution rates of different elements during linear scan voltammetry experiments on stainless steel samples via ICP-OES [1]. With the same setup, it was also possible to measure the alkaline stability of zinc phosphate conversion coatings on galvanised steel [2]. The need for a fully fledged study in coating technology is due to the fact that not the coating itself may be the rate-determining compound in corrosion protection but sometimes its corrosion products are. Chemical and electrochemical reactions can be involved and may influence each other. This is in particular true for zinc-based coatings. Systems such as Zn, Zn–Al, Zn–Mg, Zn–Ti and even ternary Zn systems (Zn–Al–Mg) show a complex reaction scheme, where the reaction depends on the exact condition of the surface at a given time. Zinc is an amphoteric metal that forms insoluble oxides and hydroxides which can be detected by impedance spectroscopy [3]. Exceeding a certain pH value may dissolve these oxides and would form zincate ions [4]. In both cases, the amount of soluble zinc can be determined using methods for analysing the electrolyte. Depending on the media, also more complex corrosion products such as simonkolleite or hydrozincate can form. In this case, the impedance characterisation can only tell about the protectiveness of the scale formed, but identification requires another method such as Raman spectroscopy to characterise a particular chemical compound.

This article is dedicated to Prof. Waldfried Plieth on the occasion of his 75th birthday.

M. Voith · A. W. Hassel (✉)
Institute for Chemical Technology of Inorganic Materials,
Johannes Kepler University,
Altenberger Str. 69,
4040 Linz, Austria
e-mail: hassel@elchem.de
URL: <http://www.jku.at/ictas>

G. Luckeneder
Research and Development, voestalpine Stahl GmbH,
voestalpine-Straße 3,
4021 Linz, Austria

In particular, for corrosion studies, the direct identification of the reaction products on the sample surface by means of *in situ* Raman spectroscopy is of interest. This was realised through an adapted design of a flow cell by Tomandl et al. [5]. This identification is not always straightforward since sometimes surprising products are found. One example is the formation of a combined scale on presshardened steels that consists of akaganeite, hydrozincite and simonkolleite [6, 7]. Presshardened steel is galvanised steel that is subsequently thermomechanically treated. This combined increase in temperature and pressure enables the formation of an intermetallic layer that would otherwise not form because zinc would evaporate before the reaction temperature for the solid–solid reaction is reached. The intermetallic layer formed in this way shows remarkably high corrosion resistance that is superior to the corrosion protection properties of the coating alone.

Recent works in the field of corrosion protection of steel with ternary systems like Zn–Mg–Al [8] lead to new methods to characterise these multiphase systems [9]. Therefore, a method was found to characterise and quantify the different coexisting phases on a Zn–Mg–Al-coated steel with an energy-dispersive X-ray technique. Also, a method was developed to follow the corrosive attack on such systems via time laps microscopy [10]. The obtained results provide information about the microstructural corrosion on multiphase systems as well as pH gradients and formed corrosion products.

Specific questions may require specific adaptations of methods which is for example the case when a systematic investigation of a composition spread sample of a binary alloy shall be studied. Based on the initial design of the scanning droplet cell microscopy, a microelectrochemical system with downstream analytics was implemented that is useful for the characterisation of dissolving metals [11, 12]. One example of its application was described for Mg–Zn material libraries in which critical compositions of the parent material could be identified which show a particular behaviour, for a specific reaction such as oxygen evolution.

The design of the cell used in this work was inspired by previous works of Ogle and Weber [1] and Sullivan et al. [10] combining the benefits of an electrochemical flow cell with downstream analytics and the possibility to observe changes on the sample surface during exposure to a flowing electrolyte.

In order to understand the behaviour of various Mg–Zn alloys, it was necessary to prepare them as bulk materials. Due to the phase diagram of this binary system, this is not straightforward; therefore, the preparation method was adapted from the work of Prosek et al. [13] which uses a simple and fast method to produce Zn–Mg alloys using pure Zn to increase the zinc content in a MgZn50

prealloy. This work was performed under inert conditions in an inductive furnace.

In this work, a novel setup is shown which couples the benefits of electrochemistry and highly sensitive analytics with a flow-through cell whose design and geometry allow the investigation of changes on sample surfaces and at the same time the detection of soluble species via downstream analytics.

Experiments

Chemicals

All chemicals used were of analytical grade, and water was deionised. The MgZn50 (50 wt%Mg and 50 wt% Zn) prealloy was provided by VOESTALPINE AG Linz. The zinc (Roth) used to produce the MgZn₂ sample was of analytical grade and has ≥ 99.99 % purity. A stock standard solution of Zn(II) of 1,000 mg l⁻¹ was prepared by dissolving 1.245 g ZnO p.a. (Merck) in 10 ml 40 % HNO₃ (Merck) and diluting with deionised water. All solutions were deaerated for at least 30 min with Argon 4.6 (Linde) prior to use.

Sample preparation

To prepare MgZn₂ samples, the MgZn50 alloy was enriched with zinc. The calculated amounts of zinc and MgZn50 alloy were put together in an alumina crucible which then was assembled into the melting chamber of an induction furnace (Linn High Therm). Before melting, the chamber was evacuated and purged with Varigon® H6 (Linde) for several times to remove remaining oxygen and avoid oxidation of the metals during the melting, casting and cooling process afterwards. The molten alloy was cast under inert conditions. Boron nitride spray was used as a separating agent on the inner walls of the mould to avoid sticking of the alloy at the walls and allow an easier release. After cooling, the released ingots were cleaned, cut into correct shape, embedded, polished and mounted into the working cell.

Experimental setup

The experimental setup scheme is shown in Fig. 1.

The setup consists of following parts:

- Working (W) and reference (R) cell
- Hitachi Z-8230 Polarized Zeeman atomic absorption spectrophotometer (AAS)
- ESA high-performance liquid chromatography pump (P)

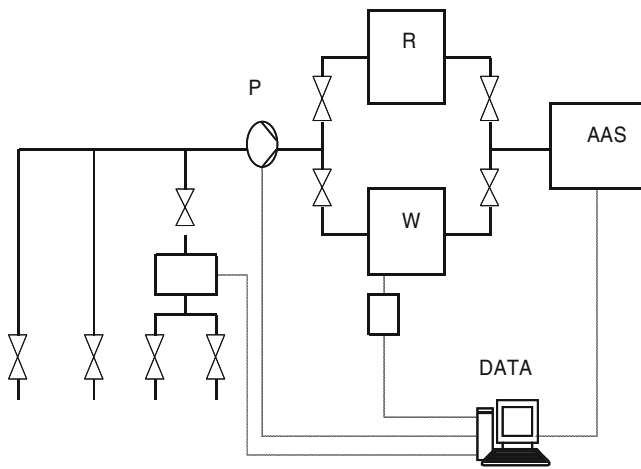


Fig. 1 Piping and instrumentation of the experimental setup

- World Precision Instruments valves (two and three way)
- Silicon rubber pipes
- Self-developed LabVIEW® interface (DATA) which allows continuous data acquisition and processing in real time during experiments
- Connections for calibrating solutions, process media and rinsing agents

Both working and reference cells are made of PTFE. The geometry of the inner chamber can be varied between $35 \times 35 \times 5$ and $35 \times 8 \times 3$ mm ($l \times w \times h$) to allow for an investigation of the influence of the cell geometry. It is also possible to adjust the flow profile with differently shaped inlays to improve the ratio between cell volume, flow rate and exposed sample surface that is exposed to the process media. Finally, the cell is sealed

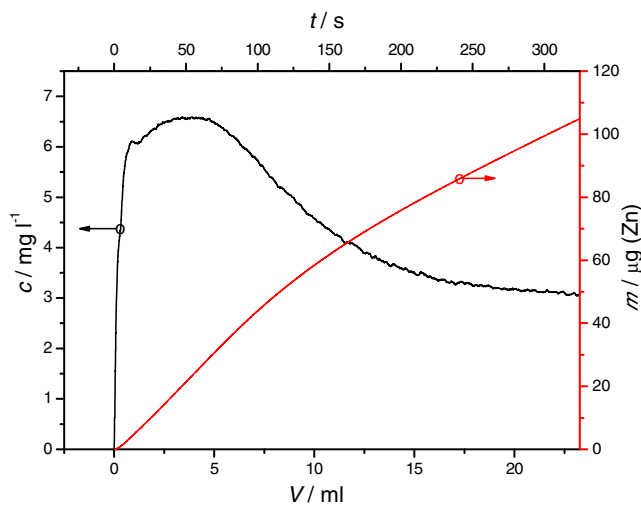


Fig. 2 Concentration curve (black) and total dissolved amount of zinc (red) during a typical flow-through experiment with HCl (0.005 M) over a MgZn_2 sample

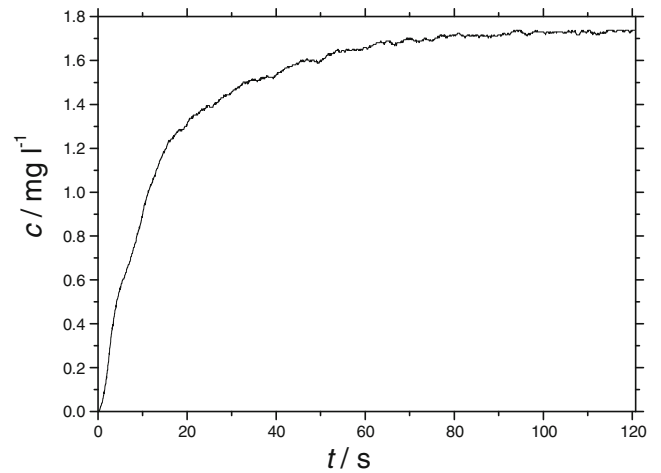


Fig. 3 Concentration over time during water replacement experiment

using an optical window that allows a direct observation using a camera or a microscope to observe possible changes on the sample surface or gas formation during exposure to the liquid media. Furthermore, the entire construction allows performing optical spectroscopy namely UV–VIS and Raman through the thin electrolyte layer.

The working and reference cells are connected in parallel providing two major benefits:

- The inner geometry of the reference and the working cells are identical, so that within a defined time span, exactly the same amount of liquid flows into the atomisation unit of the spectroscope. This is necessary to avoid failures which may occur if the flow into the AAS during calibration is not the same as during measuring.

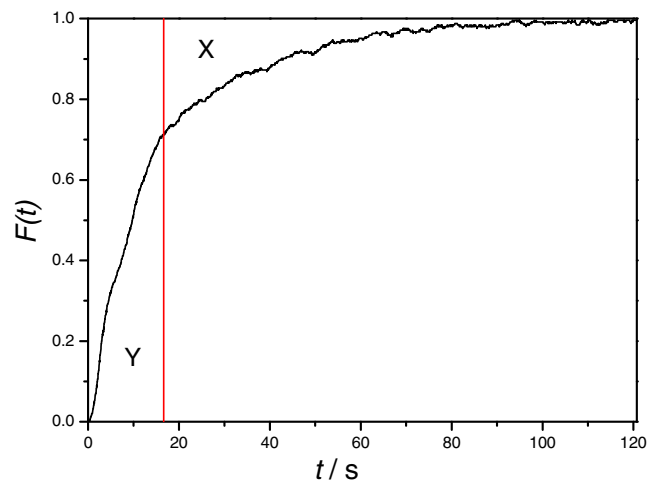


Fig. 4 Retention time sum function of a working cell with the dimensions $34 \times 19 \times 2.8$ mm ($l \times w \times h$)

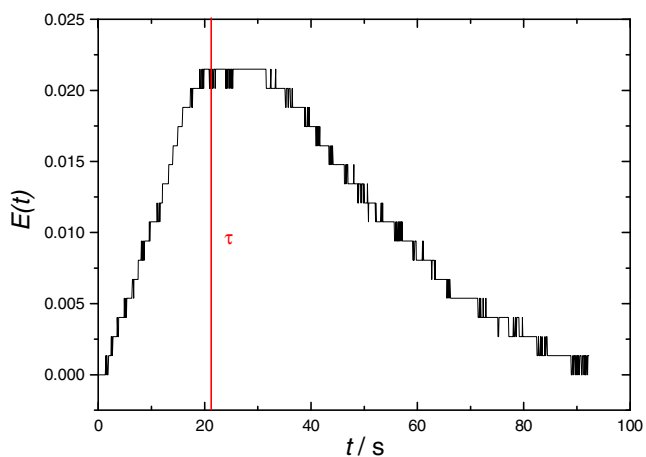


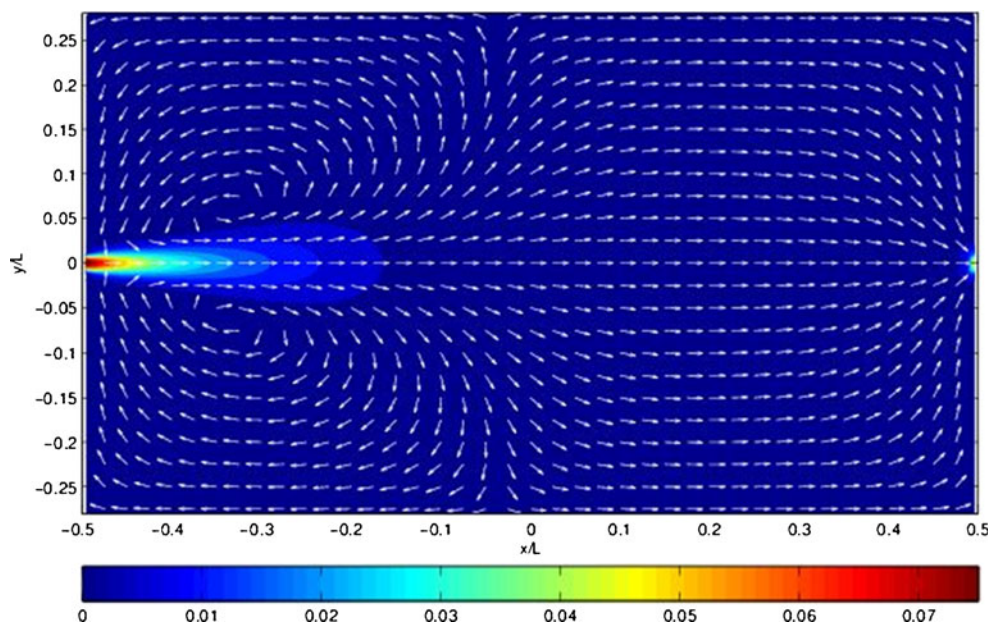
Fig. 5 Retention time density function of a working cell with the dimensions $34 \times 19 \times 2.8$ mm ($l \times w \times h$)

- By using a reference cell for calibration, the polished surface of the sample in the working cell is not contaminated with the standard solution or rinsing agents.

Procedure

The embedded and polished alloy samples are placed in the working cell. To calibrate the atomic absorption spectrophotometer and avoid contamination of the sample surface by the calibration standard solution, these are pumped through the reference cell into the AAS. After calibration, the

Fig. 6 CFD simulation of a working cell ($34 \times 19 \times 2.8$ mm). Velocity vectors coloured by velocity magnitude (in metres per second)



whole system is purged with deionised and deaerated water until the valves are switched so that the process media can flow through the working cell and into the AAS to be analysed.

Results and discussion

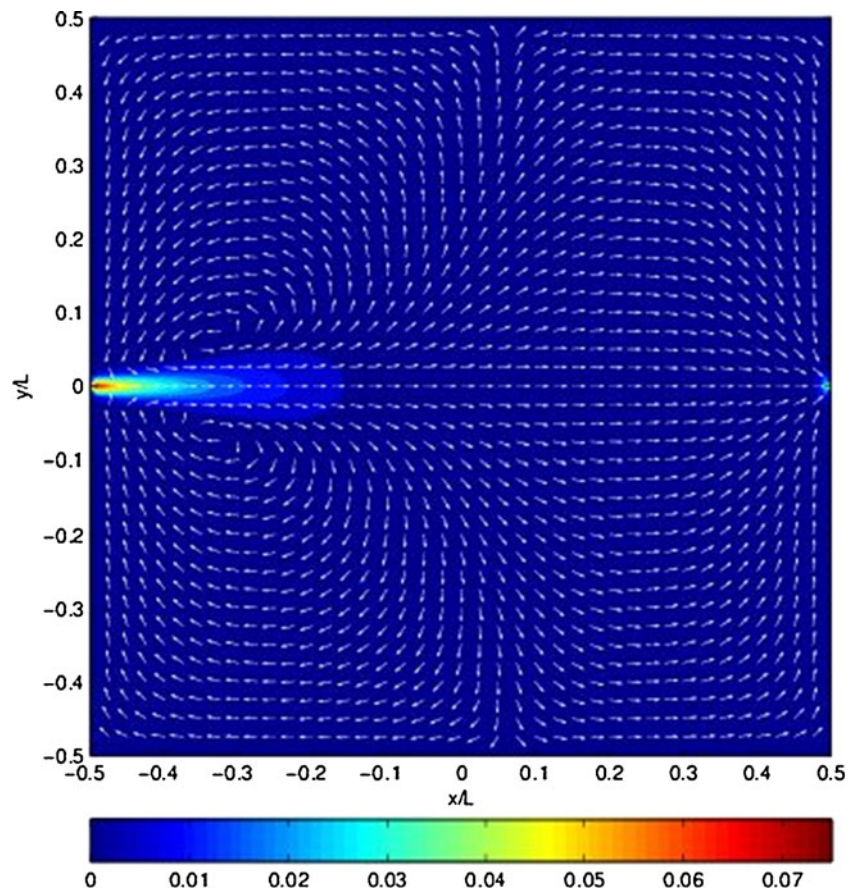
Experimental results

Figure 2 shows the concentration curve for an experiment where a MgZn_2 sample is overflowed by HCl (0.005 M) with a flow rate of 4.3 ml min^{-1} . Within the first seconds, the amount of dissolved zinc increases rapidly and reaches the maximum value after about 60 s. Due to hydrogen formation on the sample surface, the zinc concentration in the analyte decreases asymptotically. This is because the hydrogen gas bubbles block the surface and hinder access of the media to the alloy.

Hydrodynamical properties

Owing to the fact that the flow-through cell in the setup is not an ideal flow tube, backmixing will occur. This effect leads to signal peak broadening because of the elongation of the time for a particle to pass the cell (increase of average retention time). To determine the real retention time for a certain cell geometry, the water in the system is replaced by a solution of known con-

Fig. 7 CFD simulation of a working cell (34×34×2.8 mm). Velocity vectors coloured by velocity magnitude (in metres per second)



centration. Hence, the concentration curve is recorded over time until the water is completely replaced by the marker solution (Fig. 3). To determine the correct retention time, it is necessary to calculate the retention time sum function $F(t)$ [14]:

$$F(t) = \frac{c(t)}{c_{\max}} \quad (1)$$

- c_{\max} Marker concentration at the inlet
- $c(t)$ Measured marker concentration at a certain point in time t
- $F(t)$ Calculated retention time sum function

Fig. 8 CFD simulation of a working cell (34×19×2.8 mm). Velocity vectors coloured by velocity magnitude (in metres per second)

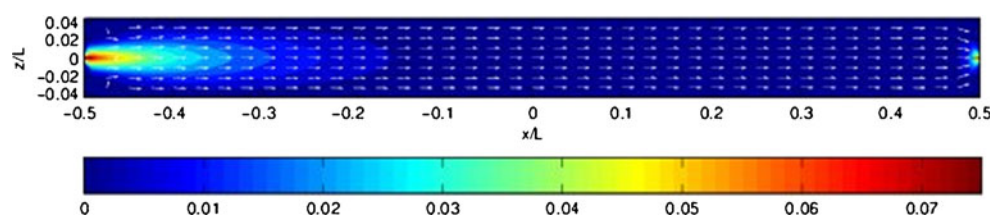


Figure 4 shows the calculated retention time sum function $F(t)$ over time t . To compute the correct retention time, the areas below and above the curve are calculated and compared. The point for which both areas X and Y are equal represents the mean retention time.

The retention time was also determined via impulse marking. Therefore, an embedded, ground and polished copper sample was electrically contacted from the back-side. A short galvanostatic pulse over 0.5 s and 10 mA released copper ions which were carried away by the flowing medium and transported into the AAS where the concentration curve was measured. By using Eqs. (2) and (3), it is possible to calculate the retention time

density function $E(t)$ as well as the retention time τ [14]:

$$E(t) = \frac{c(t)}{\int c(t)dt} \quad (2)$$

$$\tau = \int t^* E(t) dt \quad (3)$$

$c(t)$ Measured marker concentration at a certain point in time t

$E(t)$ Calculated retention time density function

τ Calculated retention time

The obtained graph for the density function over time is shown in Fig. 5. The inner geometry of the cell has a decisive influence on the liquid flow through the cell. In Figs. 6 and 7, the computational fluid dynamics (CFD) simulated velocity vectors for an aqueous media flowing through cells with different geometries at an identical flow rate of 3.5 ml min^{-1} are shown. By a comparison of the pathways through these two cells, it is seen that transport through the narrower one (Fig. 6) is faster than in the wider cell due to reduced backmixing. This results in lower retention times and significantly lower peak broadening.

Figure 8 shows the lateral view for the velocity vectors of flowing aqueous media through the cell. The absence of any turbulence demonstrates that the flow is laminar in the region where the sample is located in the cell.

Summary

In the present work, a novel flow-through cell–atomic absorption spectrophotometric system is presented. The hydrodynamical properties of the cell were determined both experimentally and using computational fluid dynamics. It is now possible to characterise and quantify soluble species in real time during an experiment in which an alloy surface comes in contact with a continuously flowing aqueous media. The construction of the cell allows not only for the integration of electrochemical techniques, e.g. using a micro reference electrode [13] but also the simultaneous application of further methods such as optical spectroscopy which results in a comprehensive characterisation of the ongoing processes. The developed data acquisition

and processing software allows to measure and compute different parameters concurrently and allows to simultaneously use various analytical and electrochemical methods.

Acknowledgments Thanks to Österreichische Forschungsförderungsgesellschaft FFG and voestalpine Stahl GmbH for the financial support of this work through grant 827517.

References

- Ogle K, Weber S (2000) Anodic dissolution of 304 stainless steel using atomic emission spectroelectrochemistry. *J Electrochem Soc* 147:1770–1780
- Ogle K, Tomandl A, Meddahi N, Wolpers M (2004) The alkaline stability of phosphate coatings I: ICP atomic emission spectroelectrochemistry. *Corros Sci* 46:979–995
- Bonk S, Wicinski M, Hassel AW, Stratmann M (2004) Electrochemical characterizations of precipitates formed on zinc in alkaline sulphate solution with increasing pH values. *Electrochem Comm* 6:800–804
- Fenster C, Rohwerder M, Hassel AW (2009) The impedance-titrator: a novel setup to perform automated pH-dependent electrochemical experiments. *Mater Corr* 60:855–858
- Tomandl A, Wolpers M, Ogle K (2004) The alkaline stability of phosphate coatings II: in situ Raman spectroscopy. *Corros Sci* 46:997–1011
- Autengruber R, Luckeneder G, Hassel AW (2012) Corrosion of press-hardened galvanized steel. *Corros Sci* 63:12–19
- Autengruber R, Luckeneder G, Hassel AW (2012) Surface and coating analysis of press-hardened hot-dip galvanized steel sheet. *Steel Res Int*. doi:srin.201200068
- Schuerz S, Fleischanderl M, Luckeneder GH, Preis K, Haunschmid T, Mori G, Kneissl AC (2009) Corrosion behaviour of Zn–Al–Mg coated steel sheet in sodium chloride-containing environment. *Corros Sci* 51:2355–2363
- Commenda C, Pühringer J (2010) Microstructural characterization and quantification of Zn–Al–Mg surface coatings. *Mater Charact* 61:943–951
- Sullivan J, Mehraban S, Elvins J (2011) In situ monitoring of the microstructural corrosion mechanisms of zinc–magnesium–aluminium alloys using time lapse microscopy. *Corros Sci* 53:2208–2215
- Klemm SO, Schauer JC, Schuhmacher B, Hassel AW (2011) A microelectrochemical scanning flow cell with downstream analytics. *Electrochim Acta* 56:4315–4321
- Klemm SO, Schauer JC, Schuhmacher B, Hassel AW (2011) High throughput electrochemical screening and dissolution monitoring of Mg–Zn material libraries. *Electrochim Acta* 56:9627–9636
- Prosek T, Nazarov A, Bexell U, Thierry D, Serak J (2008) Corrosion mechanism of model zinc–magnesium alloys in atmospheric conditions. *Corros Sci* 50:2216–2231
- Müller-Erlwein E (2007) *Chemische reaktionstechnik*. Teubner Verlag, Wiesbaden